

# Novel index-guided photonic crystal fiber surface-enhanced Raman scattering probe

He Yan,<sup>1\*</sup> Jie Liu,<sup>1</sup> Changxi Yang,<sup>1</sup> and Guofan Jin,<sup>1</sup> Claire Gu,<sup>2</sup> and Lantian Hou<sup>3</sup>

<sup>1</sup>State Key Laboratory of Precision Measurement Technology and Instruments, Department of Precision Instruments, Tsinghua University, Beijing 100084, China

<sup>2</sup>Department of Electrical Engineering, University of California, Santa Cruz, California 95064, USA

<sup>3</sup>Key Laboratory of Metastable materials science and technology, Yanshan University, Qinhuangdao 066004, China

\*Corresponding author: [yanhe00@mails.tsinghua.edu.cn](mailto:yanhe00@mails.tsinghua.edu.cn)

**Abstract:** We demonstrate a novel index-guided (IG) photonic crystal fiber (PCF) surface-enhanced Raman probe. Different from a regular PCF, the IGPCF has four big air holes inserted between the solid silica core and the photonic crystal cladding holes. The gold nanoparticles, serving as the surface enhanced Raman scattering (SERS) substrate, are either coated on the inner surface of the holes or mixed in the analyte solution in two separate experiments, respectively. The analyte solution enters the holes via the capillary effect. The excitation light propagating in the silica core interacts with the gold nanoparticles and the analyte through the evanescent wave which extends significantly into the four big holes when they are filled with liquid leading to a large interaction volume between the excitation light and the nanoparticles/analyte.

©2008 Optical Society of America

**OCIS codes:** (060.2370) Fiber optics sensors; (060.4005) Microstructured fibers; (300.6450) Spectroscopy, Raman.

---

## References and links

1. T. Ritari, J. Tuominen, H. Ludvigsen, J. C. Petersen, T. Sorensen, T. P. Hansen, and H. R. Simonsen, "Gas sensing using air-guiding photonic bandgap fibers," *Opt. Express* **12**, 4080-4087 (2004).
2. F. M. Cox, A. Argyros, and M. C. J. Large, "Liquid-filled hollow core microstructured polymer optical fiber," *Opt. Express* **14**, 4135-4140 (2006).
3. J. B. Jensen, L. H. Pedersen, P. E. Hoiby, L. B. Nielsen, T. P. Hansen, J. R. Folkenberg, J. Riishede, D. Noordegraaf, K. Nielsen, A. Carlsen, and A. Bjarklev, "Photonic crystal fiber based evanescent-wave sensor for detection of biomolecules in aqueous solutions," *Opt. Lett.* **29**, 1974-1976 (2004).
4. S. O. Konorov and A. M. Zheltikov, "Photonic-crystal fiber as a multifunctional optical sensor and sample collector," *Opt. Express* **13**, 3454-3459 (2005).
5. S. Smolka, M. Barth, and O. Benson, "Selectively coated photonic crystal fiber for highly sensitive fluorescence detection," *Appl. Phys. Lett.* **90**, 111101 (2007).
6. S. Smolka, M. Barth, and O. Benson, "Highly efficient fluorescence sensing with hollow core photonic crystal fibers," *Opt. Express*, **15**, 12783-12791 (2007).
7. S. O. Konorov, C. J. Addison, H. G. Schulze, R. F. B. Turner, and M. W. Blades, "Hollow-core photonic crystal fiber-optic probes for Raman spectroscopy," *Opt. Lett.* **31**, 1911-1913 (2006).
8. H. Yan, C. Gu, C. Yang, J. Liu, G. Jin, J. Zhang, L. Hou, and Y. Yao, "Hollow core photonic crystal fiber surface-enhanced Raman probe," *Appl. Phys. Lett.* **89**, 204101 (2006).
9. Y. Zhang, C. Shi, C. Gu, L. Seballos, and J. Z. Zhang, "Liquid core photonic crystal fiber sensor based on surface enhanced Raman scattering," *Appl. Phys. Lett.* **90**, 193504 (2007).
10. F. M. Cox, A. Argyros, M. C. J. Large, and S. Kalluri, "Surface enhanced Raman scattering in a hollow core microstructured optical fiber," *Opt. Express*, **15**, 13675-13681 (2007).
11. S. M. Nie and S. R. Emery, "Probing single molecules and single nanoparticles by surface-enhanced Raman scattering," *Science* **275**, 1102-1106 (1997).
12. K. Kneipp, Y. Wang, H. Kneipp, L. T. Perelman, I. Itzkan, R. Dasari, and M. S. Feld, "Single molecule detection using surface-enhanced Raman scattering (SERS)," *Phys. Rev. Lett.* **78**, 1667-1670 (1997).
13. K. Kneipp, H. Kneipp, I. Itzkan, R. R. Dasari, and M. S. Feld, "Surface-enhanced Raman scattering and biophysics," *J. Phys. Condens. Matter* **14**, R597-R624 (2002).
14. C. L. Haynes, C. R. Yonzon, X. Zhang, and R. P. V. Duyne, "Surface-enhanced Raman sensors: early history and the development of sensors for quantitative biowarfare agent and glucose detection," *J. Raman Spectrosc.* **36**, 471-484 (2005).
15. Y. Zhu, H. Du, and R. Bise, "Design of solid-core microstructured optical fiber with steering-wheel air cladding for optimal evanescent-field sensing," *Opt. Express* **14**, 3541 (2006).

16. T. M. Monro, W. Belardi, K. Furusawa, J. C. Baggett, N. G. R. Broderick, and D. J. Richardson, "Sensing with microstructured optical fibres," *Meas. Sci. Technol.* **12**, 854–858 (2001).
  17. J. M. Fini, "Microstructure fibres for optical sensing in gases and liquids," *Meas. Sci. Technol.* **15**, 1120–1128 (2004).
  18. Y. Zhang, C. Gu, A. M. Schwartzberg, and J. Z. Zhang, "Surface-enhanced Raman scattering sensor based on D-shaped fiber," *Appl. Phys. Lett.* **87**, 123105 (2005).
  19. D. Pristiniski and H. Du, "Solid-core photonic crystal fiber as a Raman spectroscopy platform with a silica core as an internal reference," *Opt. Lett.* **31**, 3246-3248 (2006).
  20. M. Volkan, D. L. Stokes, and T. Vo-Dinh, "Surface-enhanced Raman of dopamine and neurotransmitters using sol-gel substrates and polymer-coated fiber-optic probes," *Appl. Spectrosc.* **54**, 1842-1848 (2000).
  21. D. L. Stokes and T. Vo-Dinh, "Development of an integrated single-fiber SERS sensor," *Sens. Actuators* **69**, 28-36 (2000).
  22. E. Polwart, R. L. Keir, C. M. Davidson, W. E. Smith, and D. A. Sadler, "Novel SERS-active optical fibers prepared by the immobilization of silver colloidal particles," *Appl. Spectrosc.* **54**, 522-527 (2000).
  23. T. K. Sau and C. J. Murphy, "Self-assembly patterns formed upon solvent evaporation of Aqueous Cetyltrimethylammonium Bromide-Coated Gold Nanoparticles of various shapes," *Langmuir* **21**, 2923-2929 (2005).
  24. J. Ma and Y. Li, "Fiber Raman background study and its application in setting up optical fiber Raman probes," *Appl. Opt.* **35**, 2527-2533 (1996).
- 

## 1. Introduction

Recently, photonic crystal fibers have shown great potential in chemical, biological, and environmental detections in conjunction with absorption [1, 2], fluorescence [3-6], Raman [7] and surface enhanced Raman scattering (SERS) [8-10]. Among these techniques, SERS is particularly attractive due to its molecular specificity and huge enhancement for the Raman signal ( $10^6\sim 10^{15}$  [11-14]). On the other hand, optical fibers provide the flexibility, easy sampling, and remote sensing capability. The combination of SERS and optical fibers makes it possible for a real-time, molecule specific, compact, flexible, reliable and minimally-invasive sensing method. In addition, the holey structure of a photonic crystal fiber not only provides the bandgap for light confinement in the core, but also offers an ideal space for the nonlinear interaction between the excitation light and the sample. In a hollow core photonic crystal fiber, the sample enters the central air core and the transmitted excitation light excites the sample directly [7-9]. In an index-guided fiber, the excitation light propagates in the silica core while the evanescent wave extends into the cladding and interacts with the sample there. Therefore, it is important to design the structure of an index-guided PCF to maximize the overlap between the evanescent wave and the liquid sample [15-19]. Previously, Herry Du's group has presented a steering wheel PCF (SW-PCF) design for evanescent-field based sensing [15]. The inner layers of a solid core PCF is replaced by three large air holes and three silica bridges around the central solid core.

In this letter, we present a novel index-guided photonic crystal fiber surface-enhanced Raman probe. Different from other PCFs, this fiber has four big air holes inserted between the solid silica core and the photonic crystal cladding holes, as shown in Fig. 1. This structure is easier to fabricate than the steering wheel structure, and takes advantage of the combination of index guiding and photonic bandgap confinement mechanisms resulting in a higher energy overlap factor of the evanescent wave in the four big air holes. The gold nanoparticles serving as the surface enhanced Raman scattering (SERS) substrate, is either coated on the inner surface of the holes or mixed in the analyte solution, in two separate experiments, respectively. The analyte solution enters the holes via the capillary effect. The excitation light is coupled into the fiber from one end (measuring tip) while the sample entrance is at the other end (probing tip) of the fiber. The excitation light propagating in the silica core interacts with the gold nanoparticles and the analyte through the evanescent wave which extends significantly into the four big holes when they are filled with liquid leading to a large interaction volume between the excitation light and the nanoparticles/analyte. The SERS signal scattered by the sample propagates through the silica core back to the measuring tip, then is coupled out of the fiber into the Raman spectrometer. Comparing to a hollow core PCF SERS probe, the IGPCF SERS probe can operate at more than one excitation wavelengths due to the index-guiding nature. Comparing to other solid core PCF SERS probes [18-22], the four

big holes provide a larger volume for the interaction between the evanescent wave and the nanoparticles/analyte.

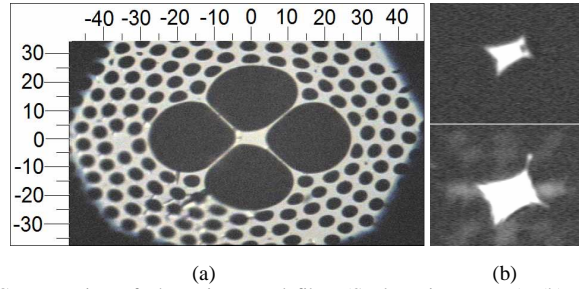


Fig. 1. (a). Cross section of photonic crystal fiber (Scale: micrometers); (b) Near-field light pattern at the exit, taken with a charge-coupled device camera with different exposures.

The photonic crystal fiber used in our experiments is fabricated in Yanshan University, China. Figure 1 shows the cross section of such a photonic crystal fiber. The central area is a silica core surrounded by four big air holes inside a periodical array of cladding air holes. The central silica core is approximately a rectangle with a length of  $\sim 10\mu\text{m}$  and a width of  $\sim 6\mu\text{m}$ ; the four big air holes have a diameter of  $\sim 20\mu\text{m}$ ; and the surrounding small air holes have an average diameter of  $\sim 2.5\mu\text{m}$  and are arranged in a triangular lattice with a  $\sim 3\mu\text{m}$  pitch. The total diameter of the fiber including the outer coating is  $\sim 300\mu\text{m}$ .

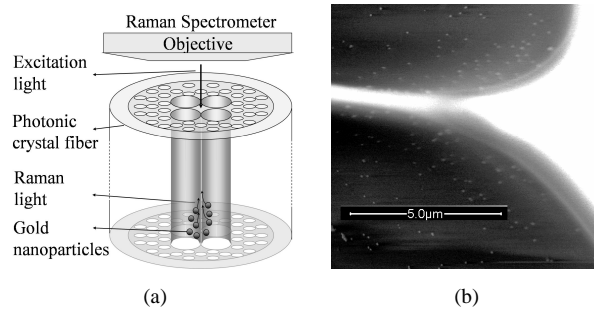


Fig. 2. (a). Schematic of the experimental setup; (b) SEM image taken from the side surface of the silica core.

## 2. Experiments

### 2.1 Gold nanoparticles coated on the inner surface of the IGPCF

The experiment was carried out in the following steps using a setup as shown in Fig. 2(a). The fiber was cut into segments of about 5 cm in length, with both ends cleaved carefully. A colloid of Au polygonal nanoparticles (the concentration is  $\sim 5 \times 10^{-11}$  M) with a diameter of  $\sim 80$  nm stabilized by a positive surfactant (CTAB, hexadecyl trimethyl ammonium bromide) was used as the SERS substrate. These nanoparticles could easily cling to the inner surface of the IGPCF by the opposite charge affinity [23]. In our first experiment, the probing-tip of the fiber was dipped into the gold nanoparticles colloid for about 5 minutes. The solution entered the air holes for about 2 cm due to the capillary effect. After drying the solution under a  $60^\circ\text{C}$  heating condition for about two hours the gold nanoparticles were attached on the inner surface of the air holes. To investigate the coating of the gold nanoparticles on the surface around the silica core, we cut such a probe at a location 15 mm above the probing end, and then observed the cross section using a SEM system. The fiber was tilted with respect to the lens axis in order to view the inside of the hole. As shown in Fig. 2(b), gold nanoparticles are attached on the surface inside the big holes outside the silica core, creating SERS active area all around the silica core. A sample of  $10^{-5}$  M Rhodamine B (RhB) solution was used to test the performance of the SERS probe. The SERS active probing-tip was dipped into the RhB

solution for 5 seconds and partially filled with the RhB solution via the capillary effect, the filling length is about 1 cm. Since the concentration of the solution is relatively low, the refractive index inside the four big holes is about the same as that of water (1.33), which is still lower than that of the silica core (1.5). Therefore, the index difference allows the excitation light to be confined in the silica core. The four big air holes actually provide a large interaction volume for the evanescent light and the solution. After taking the tip out of the RhB solution, we immediately measured the SERS spectrum from the measuring-tip using a Renishaw System RM2000 with a 632.8 nm excitation light. A 50 $\times$  objective lens was used to focus the excitation light into the silica core through the measuring-tip, and to collect the scattered Raman signal. Curve B in Fig. 3(a) shows the measured SERS signal of RhB (the IGPCF's Raman background has been subtracted,) which is agree with the result obtained on the SERS substrate coated on a silicon wafer (curve A in Fig. 3(a), the same gold nanoparticles were coated on the silicon wafer), and all the SERS peaks of RhB detected by the IGPCF SERS probe are consistent with those reported in the literature [23]. After the RhB solution dried in the holes, the SERS signal grew stronger (the result is not presented since it is the same as the former, except the intensity), for the reason that more RhB molecules were attached to the gold nanoparticles on the surface around the silica core, while most RhB molecules were in solution but not attached to the gold nanoparticles before the solution was dried. Specifically, the peak at 1648  $\text{cm}^{-1}$  increased from  $\sim 14000$  counts to  $\sim 31000$  counts after the RhB solution dried. When using a uncoated IGPCF to detect RhB solution, even with higher RhB concentration ( $10^{-4}$  M), no RhB Raman signal could be obtained either in liquid or dry sample.

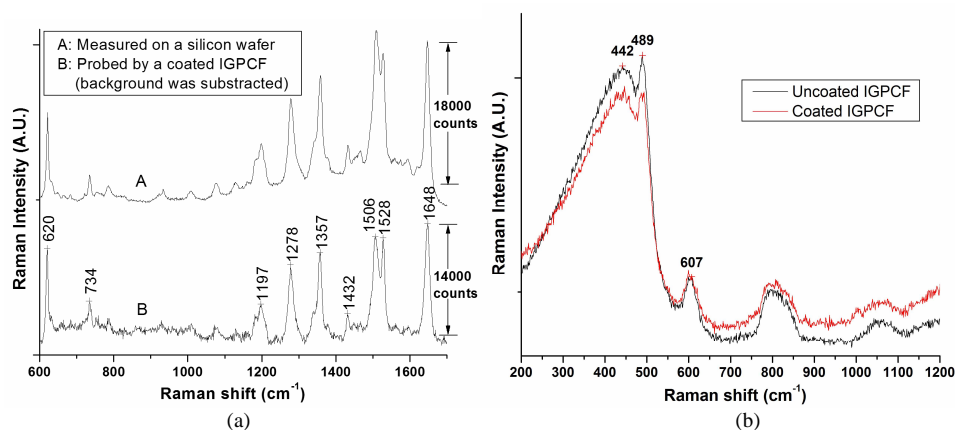


Fig. 3. (a). SERS spectrum of  $10^{-5}$ M RhB: Curve A: obtained using a SERS substrate coated on a Si wafer (excitation power 0.47 mW, scan time 20 s, and accumulation times 1); Curve B, taken with a SERS substrate coated on the inner surface of the IGPCF holes. (Excitation power 4.7mW; scan time 10s; accumulation times 3); (b) Raman backgrounds of uncoated and coated IGPCF.

The IGPCF has a Raman background due to the interaction between the excitation light and the silica core (as shown in Fig. 3(b)) [24]. The background of silica is mainly located in the range from 200 to 900  $\text{cm}^{-1}$ , while most SERS peaks of RhB spread from 1200 to 1700  $\text{cm}^{-1}$ . The Raman backgrounds of an IGPCF were measured before and after the coating process, as shown in Fig. 3(b). The two spectra are similar to each other. The nanoparticles coated on the inter surface did not enhance the IGPCF background.

## 2.2 Gold nanoparticles mixed with the analyte

To involve more nanoparticles/analyte in the SERS activity, we carried out a second experiment in which uncoated IGPCFs were used to detect mixed solutions of the gold nanoparticles colloid and the analyte. It is different from the first experiment since the gold nanoparticles are not attached to the surface outside the silica core but mixed with the RhB

molecules in solution leading to higher intensity inside the liquid filled big holes. A RhB solution ( $10^{-4}$  M) was diluted by the same gold nanoparticles colloid as that used in the first experiment to obtain various concentration mixtures of RhB molecules ( $10^{-5}$  M~ $10^{-7}$  M), thus the concentrations of gold nanoparticles in the mixtures are close to  $5 \times 10^{-11}$  M. Three uncoated 5 cm length IGPCFs were dipped into the three nanoparticles/RhB mixed solutions separately for 5 seconds. The mixed solution entered the air holes about 1 cm via the capillary effect. Then the probe was measured by the Raman spectrometer. Figure 4 shows the measured SERS spectra, which are also consistent with previous experiments. By this method, the detection limitation is down to  $10^{-7}$  M (curve C in Fig. 4(a)), this concentration mixture was also measured directly by the Raman spectrometer under the same excitation power and scan time, but no RhB signal could be obtained.

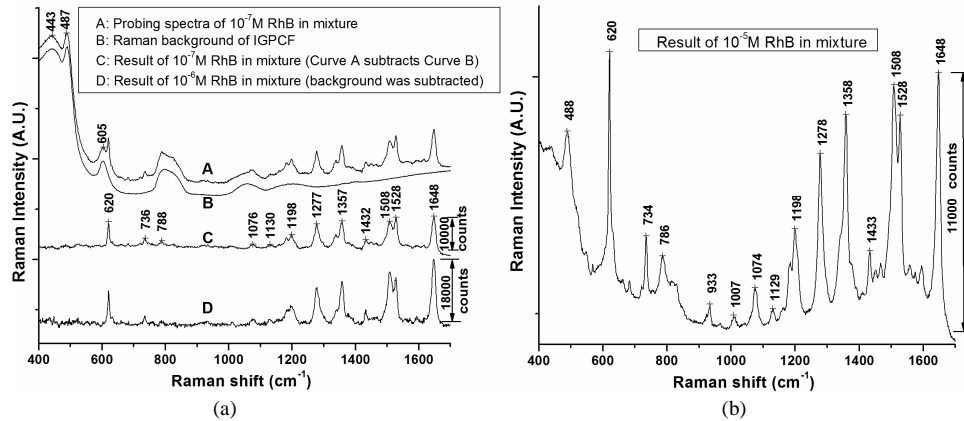


Fig. 4. (a). Curve A: SERS spectrum of  $10^{-7}$  M RhB mixed with gold nanoparticles (excitation power 4.7 mW; scan time 10 s; accumulation times 3). Curve B: the IGPCF background. Curve C: Subtraction between Curve A and Curve B. Curve D: SERS spectrum of  $10^{-6}$  M RhB mixed with gold nanoparticles (background was subtracted, excitation power 4.7 mW; scan time 10 s; accumulation times 3); (b). SERS spectrum of  $10^{-5}$  M RhB mixed with gold nanoparticles (excitation power 4.7 mW; scan time 10 s; accumulation times 1).

The intensity of the peak at  $1648 \text{ cm}^{-1}$  is about 10000, 18000 and 33000 counts respectively while the concentration of RhB is  $10^{-7}$  M,  $10^{-6}$  M and  $10^{-5}$  M (the result of  $10^{-5}$  M RhB should multiply 3 since it only accumulated once). In Fig. 4(b), the peak at  $488 \text{ cm}^{-1}$  is corresponding to the silica background (as shown in Fig. 3(b) and Curve B in Fig. 4(a)). In comparison with the experiment that the gold nanoparticles were coated on the inner surface of the IGPCF, the mixture detection can reach lower concentration for the reason that in the mixture solution the gold nanoparticles were distributed in the solution in the four big air holes to attach more analyte molecules, leading to higher sensitivity.

### 3. Calculation of the light distribution in the IGPCF

To verify the light confinement inside the solid core and provide guidelines for further improvement of such an IGPCF SERS probe, we theoretically analyzed the IGPCF with the MIT photonic-bands (MPB) code. In our simulation, the parameters were labeled as: air hole diameter  $d$ , pitch  $\Lambda$ , and the diameter of the four big holes  $d_1$ . Mode profile and energy overlap factor, defined as the percentage of energy propagating in the four big holes with respect to total mode energy, were calculated. We varied the geometric parameters in our calculation and found that the energy overlap factor increased with the increase of  $d_1/\Lambda$ , but was not sensitive to the change of  $d/\Lambda$ . When the diameter of the central core is much larger than the wavelength of light, the index guiding mechanism is dominant and the outer holes contribute little to the core guiding. On the other hand, to achieve higher energy overlap,  $d_1/\Lambda$  is increased and the core becomes smaller until its diameter is equal to or even smaller than the wavelength of light. In this situation, much energy would spread to the glass bridges

around the core, finally leading to unconfinement. Therefore, the outer cladding holes are necessary to confine the light in the central core by both total internal reflection and photonic band gap mechanisms, in cases both with and without liquid. Figure 5 shows light confinement when the holes are either empty (Fig. 5(a)) or filled with liquid (Fig. 5(b)). The parameters used in Fig. 5 are:  $d/\Lambda = 0.8$ ,  $d_1/\Lambda = 2.6$ ,  $\Lambda = 1\mu\text{m}$  and the wavelength is 632.8nm. The energy overlap factor in Fig. 5(a) is 0.0042, and that in Fig. 5(b) is 0.0203. If we increase  $d/\Lambda$  to 0.9 and  $d_1/\Lambda$  to 3, the energy overlap factor can reach 0.0939 without liquid and 0.2145 with liquid, which promises an efficient usage of the excitation light. In comparison, the light intensity overlap in air holes of Henry Du's SW-PCF design [15] is 7.2%, 13.7% and 29% at 850nm, 1000nm, and 1500nm wavelength respectively.

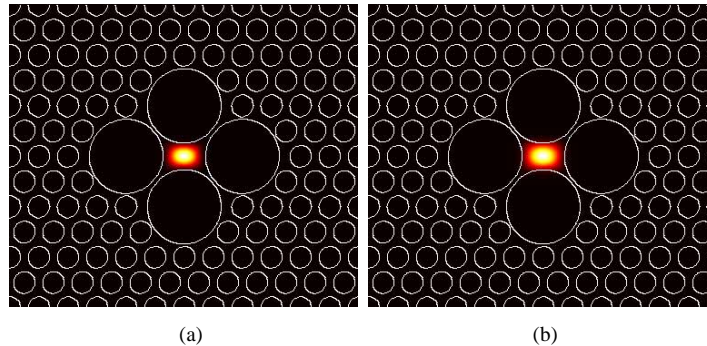


Fig. 5. Simulation results of the mode profiles of the photonic crystal fiber with  $d/\Lambda = 0.8$ ,  $d_1/\Lambda = 2.6$ ,  $\Lambda = 1\mu\text{m}$ . (a) holes are filled with air; (b) holes are filled with water.

In fact, due to our limited fiber fabrication process, the parameters of the PCF used in our experiments were not optimized. The total insertion loss of the fiber including both the coupling loss and the transmission loss was 7.4 dB. Future improvement, according to the optimized parameters, of the fiber quality will increase the sensitivity of the IGPCF SERS probe.

#### 4. Conclusion

In conclusion, we have demonstrated a robust, easy to fabricate index-guided PCF SERS probe. The four big air holes inserted between the solid silica core and the photonic crystal cladding holes provide efficient volumes for the interaction between the evanescent wave and the nanoparticles/analyte and stronger evanescent wave is excited when they are filled with liquid, resulting in a good SERS activity. The numerical results show that the energy overlap factor can reach as high as 21.45% which promises an efficient usage of the excitation light. The experimental results show that this novel photonic crystal fiber structure provides a promising platform for SERS sensors.

#### Acknowledgments

This work is financially supported in part by National Basic Research Program of China (No. 2007CB307002) and the National Natural Science Foundation of China (60678032).